JOURNAL OF COMPUTATIONAL PHYSICS 2, 149-172 (1967)

Numerical Solution of the Quasilinear Poisson Equation in a Nonuniform Triangle Mesh[1]

ALAN M. WINSLOW

Lawrence Radiation Laboratory, Livermore, California

ABSTRACT

A finite-difference method using a nonuniform triangle mesh is described for the numerical solution of the nonlinear two-dimensional Poisson equation $\nabla \cdot (\lambda \nabla \varphi) + S = 0$, where λ is a function of φ or its derivatives, S is a function of position, and φ or its normal derivative is specified on the boundary. The finite-difference equations are solved by successive overrelaxation. The triangle mesh, which is constructed numerically by solving Laplace's equation, is easily adapted to nonrectangular boundaries and interfaces. Examples of numerical results are given for the magnetostatic problem with iron, and other possible applications are mentioned.

1. INTRODUCTION

The advantages of a general triangle mesh for the numerical solution of partial differential equations in two dimensions were first pointed out in 1943 [1], and calculations by hand [2] or by electric analog computer [3] using this type of mesh were followed by digital computer applications [4–7]. The finite-difference equations given in [5], which were developed to solve parabolic equations by the alternating direction method, are adapted in this paper to the solution of elliptic equations by the method of successive overrelaxation.

In the following sections we state the basic assumptions, derive the difference equations, discuss methods for their solution, and present numerical results from an application to the two-dimensional magnetostatic problem with iron. Other

[1] This work was performed under the auspices of the U.S. Atomic Energy Commission.

applications are also mentioned, and in an appendix a numerical method is described for constructing the nonuniform mesh by solving a boundary-value problem based on Laplace's equation.

2. Description of the Method

The generalized Poisson equation

$$\nabla \cdot (\lambda \nabla \varphi) + S = 0 \tag{1}$$

is to be solved over a region R where λ is a positive function of the rectangular coordinates x, y, and may also depend on φ or its derivatives, and S is a given function of x, y. The boundary conditions are taken to be of the form $a + b\,\partial\varphi/\partial n = c$, where $\partial\varphi/\partial n$ is the normal derivative and a, b, c are constants that may take on different values over different portions of the boundary. The dependent variable φ is assumed to be continuous over R, and the quantities λ, S are assumed to be continuous over subregions of R, so that there may be interfaces at which λ and S are discontinuous; at such interfaces, $\lambda(\partial\varphi/\partial n)$ is assumed to be continuous.

The basic assumptions of the finite-difference method are: (a) the boundaries and interfaces of the region R are approximated by straight-line segments; (b) the region is triangulated; (c) the values of φ are defined at triangle vertices, and φ is assumed to vary linearly over each triangle; and (*d*) λ and S are assumed to be constant over each triangle.

The type of triangulation used here is topologically regular; that is, it is topologically equivalent to an equilateral triangle array in which six triangles meet at every interior mesh point. Since any polygonal region can be triangulated, the method can be applied to regions of any shape and will produce a mesh in which boundaries and interfaces lie entirely on mesh lines. This causes a considerable simplification in the finite difference equations and in the specification of boundary conditions.

3. Derivation of the Difference Equations

In order to establish different properties of the finite-difference equations, we give two different derivations based on the assumptions of Section II.

Integral Derivation [5]

Instead of Eq. (1), let us consider the nonlinear diffusion equation

$$c\frac{\partial\varphi}{\partial t} = \nabla \cdot (\lambda\nabla\varphi) + S, \tag{2}$$

where t represents time, and the positive coefficient c, like λ, may be a function of φ. For a steady state, (2) reduces to (1).

Consider an interior mesh point in a triangle mesh in which the assumptions of Section II hold. Associated with the primary triangle mesh we define a secondary mesh of 12-sided figures whose vertices are alternately the centroids of the six adjacent triangles and the midpoints of the six adjacent sides. This is shown in Fig. 1, in which a single such figure is shaded. The secondary mesh element

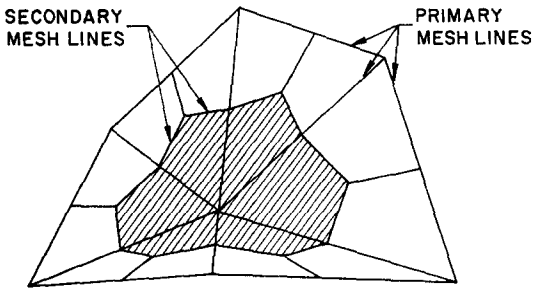

FIG. 1. Primary and secondary mesh lines.

surrounding a given vertex includes one-third of the area of each of the six primary mesh triangles sharing that vertex, so that each triangle of area A is divided into three equal quadrilaterals of area $a = A/3$.

Consider the triangle $i + \frac{1}{2}$ defined by the two side vectors $\mathbf{s}_i$, $\mathbf{s}_{i+1}$, with values $\varphi_i, \varphi_{i+1}, \varphi$ at the respective vertices as shown in Fig. 2. Since φ is assumed to be a linear function of position, each such triangle has a vector $\nabla\varphi_{i+1/2}$ associated with it which satisfies the equation

$$\varphi_j = \varphi + \mathbf{s}_j \cdot \nabla\varphi_{i+1/2} \qquad j = i, i+1 \tag{3}$$

and is given by

$$\nabla\varphi_{i+1/2} = \frac{(\varphi_i - \varphi)\mathbf{s}_{i+1}^\dagger - (\varphi_{i+1} - \varphi)\mathbf{s}_i^\dagger}{\mathbf{s}_i \cdot \mathbf{s}_{i+1}^\dagger}, \tag{4}$$

where the vector $\mathbf{s}^\dagger$ represents the vector $\mathbf{s}$ rotated clockwise by an angle $\pi/2$.

Within each triangle the flux of the diffusing quantity is given by

$$\mathbf{F}_{i+1/2} = -\lambda_{i+1/2}\nabla\varphi_{i+1/2}\,.$$

The conservation law can be expressed through Gauss' theorem by equating the surface integral of the left side of Eq. (2) over the secondary mesh element to the

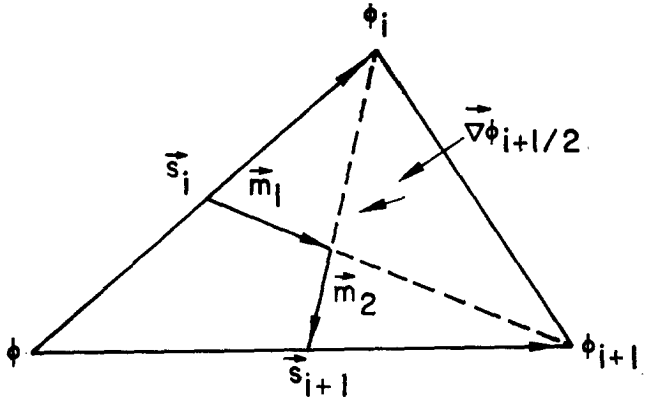

FIG. 2. Vectors used in flux calculation.

integral of the normal component of $\mathbf{F}$ over the boundary of the secondary mesh element, added to the surface integral of S.

The flux contribution $R_{i+1/2}$ from the triangle $i + 1/2$ shown in Fig. 2 to the rate of change R in the secondary mesh element is

$$R_{i+1/2} = \mathbf{F}_{i+1/2} \cdot (\mathbf{m}_1^{\dagger} + \mathbf{m}_2^{\dagger}) = \tfrac{1}{2}\,\mathbf{F}_{i+1/2} \cdot (\mathbf{s}_{i+1}^{\dagger} - \mathbf{s}_i^{\dagger}).$$

Summing around the vertex and using the central vertex value φ as the average value over the dodecagon, we obtain

$$\sum_{i=1}^{6} c_{i+1/2}\frac{\Delta\varphi_{i+1/2}}{\Delta t}a_{i+1/2} \approx \frac{\Delta\varphi}{\Delta t}\sum_{i=1}^{6} c_{i+1/2}a_{i+1/2}$$

$$= -\sum_{i=1}^{6} \mathbf{F}_{i+1/2}\frac{1}{2}(\mathbf{s}_{i+1}^{\dagger} - \mathbf{s}_i^{\dagger}) + \sum_{i=1}^{6} S_{i+1/2}a_{i+1/2}$$

or

$$\Delta\varphi = \frac{\Delta t\left[-\sum_{i=1}^{6} \mathbf{F}_{i+1/2} \cdot \frac{1}{2}(\mathbf{s}_{i+1}^{\dagger} - \mathbf{s}_i^{\dagger}) + S\right]}{G}, \tag{5}$$

where

$$G = \sum_{i=1}^{6} c_{i+1/2} a_{i+1/2} ,$$
$$S = \sum_{i=1}^{6} S_{i+1/2} a_{i+1/2} . \tag{6}$$

Using (4), and letting $\psi_i = \varphi_i - \varphi$, we can express the flux sum in Eq. (5) as

$$F = \frac{1}{2} \sum_i \frac{\lambda_{i+1/2}[(\psi_i \mathbf{s}_{i+1}^\dagger - \psi_{i+1}\mathbf{s}_i^\dagger) \cdot (\mathbf{s}_{i+1}^\dagger - \mathbf{s}_i^\dagger)]}{\mathbf{s}_i^\dagger \cdot \mathbf{s}_{i+1}}$$
$$= \frac{1}{2} \sum_i \frac{\lambda_{i+1/2}[\psi_i \mathbf{s}_{i+1} \cdot (\mathbf{s}_{i+1} - \mathbf{s}_i) + \psi_{i+1}\mathbf{s}_i \cdot (\mathbf{s}_i - \mathbf{s}_{i+1})]}{\mathbf{s}_i^\dagger \cdot \mathbf{s}_{i+1}}$$

where we have made use of the relations $\mathbf{u}^\dagger \cdot \mathbf{v}^\dagger = \mathbf{u} \cdot \mathbf{v}$ and $\mathbf{u} \cdot \mathbf{v}^\dagger = -\mathbf{u}^\dagger \cdot \mathbf{v}$. Since the sum is cyclic, we can reduce the index by one in the second term, obtaining

$$F = \frac{1}{2} \sum_i \left[\frac{\lambda_{i+1/2}}{\mathbf{s}_i^\dagger \cdot \mathbf{s}_{i+1}} \mathbf{s}_{i+1} \cdot (\mathbf{s}_{i+1} - \mathbf{s}_i) + \frac{\lambda_{i-1/2}}{\mathbf{s}_{i-1}^\dagger \cdot \mathbf{s}_i} \mathbf{s}_{i-1} \cdot (\mathbf{s}_{i-1} - \mathbf{s}_i) \right] \psi_i$$
$$= \sum_i w_i(\varphi_i - \varphi). \tag{7}$$

The coefficient of ψ_i in (7) is called the coupling coefficient for the line joining the vertex i and the center. It depends only on the nature of the two triangles having this as a common side, and can be written

$$w_i = \tfrac{1}{2} (\lambda_{i+1/2} \cot \theta_{i+1/2} + \lambda_{i-1/2} \cot \theta_{i-1/2}) , \tag{8}$$

where the angles $\theta_{i\pm1/2}$ lie opposite the side i. We note that the coupling between two points x_1 , y_1 and x_2 , y_2 is symmetric, so that

$$w_{12} = w_{21} . \tag{9}$$

Moreover, w_i can be positive, negative, or zero, but the sum of the couplings around a given point is positive:

$$\sum_{i=1}^{6} w_i = \frac{1}{4} \sum_i \frac{\lambda_{i+1/2}}{A_{i+1/2}} (\mathbf{s}_{i+1} - \mathbf{s}_i)^2, \tag{10}$$

since $\mathbf{s}_i^\dagger \cdot \mathbf{s}_{i+1} = 2A_{i+1/2}$.

Thus, Eq. (2) can be written in finite-difference approximation

$$\frac{\Delta\varphi}{\Delta t} = \frac{1}{G}\left[\sum_{i=1}^{6} w_i(\varphi_i - \varphi) + S\right] \tag{11}$$

so that for a steady state the finite-difference analog of (1) is

$$\sum_i w_i(\varphi_i - \varphi) + S = 0\,. \tag{12}$$

The continuity properties of the finite-difference solution are: (a) φ is continuous; (b) $(\nabla\varphi)_t$ is continuous; (c) $(\lambda\nabla\varphi)_n$ is continuous, where t and n refer to tangential and normal components, respectively. Statement (a) follows from assumption (c) of Section I, and (b) follows from the expression (4) for $\nabla\varphi$. Statement (c) is a consequence of our derivation by means of Gauss' theorem together with (7) which shows that the normal components of the fluxes have been replaced by mesh currents $w_i(\varphi_i - \varphi)$ flowing along mesh lines; conservation of these currents is guaranteed by (9).

Boundary points are treated in the same manner as interior points except that the coefficient λ of material outside the boundary is set equal to zero. If the outward normal gradient $\partial\varphi/\partial n$ is prescribed at a boundary, we add an external current I_j at each surface point j given by

$$I_j = \left[\frac{\partial\varphi}{\partial n}\right]_j \frac{1}{2}\left(\lambda_{j-1/2}s_{j-1/2} + \lambda_{j+1/2}s_{j+1/2}\right)$$

where $1/2(s_{j-1/2} + s_{i+1/2})$ is the length of boundary associated with the boundary point and $\lambda_{j\pm1/2}$ are the coefficients of the associated triangles.

Variational Derivation [1, 6, 7, 8]

Consider the integral

$$I(\varphi) = \frac{1}{2}\iint_R [\lambda(\varphi')\,(\nabla\varphi)^2 - 2S\varphi]dxdy\,, \tag{13}$$

where φ, λ, and S satisfy the conditions of Section II. Using a restricted variation [9] in which φ' is held fixed, with the auxiliary condition $\varphi' = \varphi$, Eq. (1) is the Euler equation for (13), so that $I(\varphi)$ will be minimized if φ satisfies (1).

Given a triangulation of the region over which φ is to be found, we can derive the finite difference equations from (13) by an adaption of the Ritz variational method. Let $\alpha_i(x,y)$ be a so-called pyramid function [10] which takes on the value

1 at the mesh point (x_i, y_i), the value zero at the nearest-neighbor mesh points, and varies linearly with position. Then if $u(x_i, y_i)$ is the value of u at the mesh point (x_i, y_i),

$$u = \sum_{\text{all } i} \alpha_i(x,y)u(x_i, y_i) \tag{14}$$

is a continuous, piecewise linear function which takes on the values of u at mesh points and satisfies the assumptions of Section II. Substituting u for φ in (13), we minimize $I(u)$ by setting $\partial I/\partial u = 0$ at each mesh point, thus obtaining the finite-difference equations as the minimum conditions for the integral (13).

From the first term in (13) we find

$$\frac{1}{2}\frac{\partial}{\partial u}(\nabla u)^2 = \nabla\alpha \cdot \nabla u .$$

Making use of (4) and

$$\nabla\alpha_{i+1/2} = \frac{1}{2A_{i+1/2}}(\mathbf{s}_i^{\dagger} - \mathbf{s}_{i+1}^{\dagger})$$

we get as the contribution to $\partial I/\partial u$ from the first term

$$\left(\frac{\partial I}{\partial u}\right)_1 = \sum_i \iint (\lambda\nabla\alpha \cdot \nabla u)_{i+1/2}dxdy = -\sum_{i=1}^{6} w_i(u_i - u),$$

where the w_i are the same coupling coefficients as before, and the last sum is over the nearest neighbors of a given mesh point.

From the second term in (13) we obtain

$$\left(\frac{\partial I}{\partial u}\right)_2 = -\sum_i S_{i+1/2}\iint \alpha_i dxdy = -\frac{1}{3}\sum_{i=1}^{6} S_{i+1/2}A_{i+1/2} . \tag{15}$$

Setting $(\partial I/\partial u)_1 + (\partial I/\partial u)_2 = 0$ we get

$$\sum_i w_i(u_i - u) + \tfrac{1}{3}\sum_i S_{i+1/2}A_{i+1/2} = 0 \tag{16}$$

as before (12).

We note from (15) that the assignment of one-third of the area of a triangle to each source density $S_{i+1/2}$ is the consequence of our assumption that u varies linearly with position, rather than appearing as the result of an arbitrary partitioning of each triangle as in the previous derivation.

4. Numerical Solution of the Difference Equations

For the linear case of (1), where λ is independent of φ, the corresponding difference equations (12) are linear in φ. The coefficient matrix w_i can be shown to be positive-definite [7], and the usual methods of successive overrelaxation can be used to solve (12). The use of this method for nonlinear problems has been justified mathematically only for certain cases [11], but we have found that the iterative methods described below converge when (1) is elliptic, provided extreme mesh distortions are avoided.

Linearized Overrelaxation

Let us first assume that (1) is linear. Solving (16) for u at a given mesh point, we get for the $(n+1)$st iteration

$$u^{n+1} = \frac{\sum_i w_i u_i^n + S}{\sum_i w_i} \tag{17}$$

where the denominator is positive by (10). Introducing the overrelaxation parameter ω $(0 < \omega < 2)$ we have

$$u^{n+1} = u^n + \omega \left(\frac{\sum_i w_i u_i^{n_i, n+1} + S}{\sum_i w_i} - u^n \right)$$

or

$$u^{n+1} = u^n + \frac{\omega}{\sum_i w_i} \left[\sum_i w_i (u_i^{n_i, n+1} - u^n) + S \right]. \tag{18}$$

In each iteration cycle the mesh points are swept in sequence, the nearest-neighbor values $u_i^{n_i, n+1}$ representing u_i^{n+1} if it already has been calculated, or u_i^n.

If now we let λ be a function of u or of its derivatives, so that the w_i are functions of u, then, depending on the rate of change of λ with u, the equations (18) can become unstable. We can maintain stability, however, by linearizing the problem in the following way [12]: (a) recalculate the w_i in (18) before each cycle; (b) underrelax the newly calculated values w_i^{new}, giving

$$w_i^{n_i+1} = \varrho w_i^{\text{new}} + (1 - \varrho) w_i^{n_i}, \tag{19}$$

where $0 < \varrho < 1$, to be used in calculating u^{n+1} by means of (18). Thus the non-

linear problem is replaced by a sequence of linear problems whose solutions have been found to converge to the solution of the original problem provided ϱ is sufficiently small.

The value of ω used in nonlinear regions is usually close to one, for reasons of stability. In linear regions, however, it is important to choose ω to optimize the convergence rate η, defined as

$$\eta^n = \left[\frac{\sum_i (u_i^{n+1} - u_i^n)^2}{\sum_i (u_i^n - u_i^{n-1})^2} \right]^{1/2} \tag{20}$$

summed over the whole mesh. Since the coefficient matrix in (18) is block tridiagonal (though not two-cyclic), analogy with the ordinary theory of successive overrelaxation suggests using the optimum value ω_{opt} given by

$$\omega_{\text{opt}} = \frac{2}{1 + (1 - \lambda^2)^{1/2}} \tag{21}$$

where, for a given ω (less than ω_{opt}) and the resulting η, we can obtain λ from the relation

$$\lambda = \frac{\omega + \eta - 1}{\omega \sqrt{\eta}} . \tag{22}$$

By choosing different values of ω and observing the corresponding asymptotic values of η, we have found that, for a linear problem, (22) holds to a high degree of accuracy, yielding values of λ that are constant to five significant figures.

For nonlinear as well as linear problems we have been able to combine (20), (21), and (22) into a satisfactory automatic scheme for optimizing ω by recalculating it every cycle in the following way: given ω^n and η^n, we have

$$\lambda = \frac{\omega^n + \eta^n - 1}{\omega^n \sqrt{\eta^n}},$$

$$\omega'_{\text{opt}} = \frac{2}{1 + (1 - \lambda^2)^{1/2}} - \omega_0 , \tag{23}$$

and

$$\omega^{n+1} = \beta\, \omega'_{\text{opt}} + (1 - \beta)\omega^n.$$

The constant $\omega_0 \approx .01$ is often useful in nonlinear problems in permitting ω to decrease when necessary, although as in linear problems it is better to have ω

somewhat too large than too small. The constant $\beta \approx .05$ underrelaxes ω so that its changes do not appreciably perturb η. Occasionally η may be greater than 1; we then hold ω constant until η has been less than 1 for a certain number ($\sim$ 5–15) of cycles, after which we resume the automatic optimization.

The dimensionless quantity

$$\varepsilon^{n+1} = \left[\frac{\sum_i (u_i^{n+1} - u_i^n)^2}{\sum_i (u_i^{n+1})^2} \right]^{1/2},$$

summed over all i, is used to test for convergence. We require $\varepsilon^{n+1} < \varepsilon_0$, where usually $\varepsilon_0 = 10^{-6}$ or 10^{-7}. A better test, based on extrapolation with constant η, would be $\varepsilon^{n+1} < \varepsilon_0(1 - \eta^{n+1})$.

Nonlinear Overrelaxation

The set of simultaneous nonlinear equations

$$F(u) = \sum_i w_i(u_i - u) + S = 0 \tag{24}$$

can be solved by replacing them by a sequence of nonlinear equations (17) in which the six neighboring values u_i of a given vertex are held fixed and each equation is regarded as a nonlinear equation in the single variable u belonging to that vertex, the dependence of the w_i on u being explicitly taken into account. As each new value is obtained, it is substituted for the old value.

For the solution of such nonlinear equations in a single variable, various iterative methods are available. Perhaps the best known are Newton's method and Aitken's δ^2 method.

Newton's Method [13, 14]

Solving (24) by Newton's method, one iteration gives

$$u^{n+1} = u^n - \frac{F^n}{(\partial F/\partial u)^n}.$$

Introducing the overrelaxation factor ω in the usual way, one iteration at each vertex yields the sequence of equations

$$u_k^{n+1} = u_k^n - \omega \frac{F_k(u^{n+1}, u^{n+1}, \ldots, u_{k-1}^{n+1}, u_k^n, \ldots, u_N^n)}{\dfrac{\partial F_k}{\partial u_k}(u^{n+1}, u^{n+1}, \ldots, u_{k-1}^{n+1}, u_k^n, \ldots, u_N^n)}, \quad (k = 1, 2, \ldots N) \tag{25}$$

where N is the number of mesh points.

Aitken's δ^2 Method [15]

The set of simultaneous equations (17) can be written

$$u = f(u). \tag{26}$$

The Aitken process consists of using (26) twice followed by a linear interpolation. Starting with a value u_k^n, we have

$$u_k^* = f(u_k^n),$$
$$u_k^{**} = f(u_k^*),$$

leading to the sequence

$$u_k^{n+1} = u_k^n - \omega \frac{(u_k^* - u_k^n)^2}{u_k^n - 2u_k^* + u_k^{**}}, \quad (k = 1, 2, \ldots N), \tag{27}$$

where we have again introduced the overrelaxation factor ω. This method requires evaluation of $f(u)$ twice at each vertex, while Newton's method requires evaluation of $F(u)$ and $\partial F/\partial u$.

5. Application to Magnetostatic Problems

Plane magnetostatic problems containing iron, because of their strong nonlinearity, provide a good example of the usefulness of the method. It is well known that such problems can be put in the form of Eq. (1) by use of the magnetic vector potential. Consider an arbitrary distribution of infinite straight parallel conductors carrying constant currents parallel to the z-axis. The magnetic field $\mathbf{H}(x,y)$ and the magnetic induction $\mathbf{B}(x,y)$ have components only in the x,y-plane while the current density $\mathbf{j}$ and magnetic vector potential $\mathbf{A}$ have only z-components which we label simply $j(x,y)$ and $A(x,y)$.

From the relations $\mathbf{B} = \mu\mathbf{H} = \nabla \times \mathbf{A}$ and $\nabla \times \mathbf{H} = 4\pi\mathbf{j}$, where $\mu(x,y,B)$ is the magnetic permeability and $B = |\mathbf{B}|$, we obtain

$$\nabla \times \left(\frac{1}{\mu}\nabla + \mathbf{A}\right) = 4\pi \mathbf{j}\,. \tag{28}$$

Because of the single-component nature of **A** and **j**, (28) reduces to

$$\nabla \cdot (\gamma \nabla A) = -4\pi j \tag{29}$$

where $\gamma \equiv \mu^{-1}$. Since $|\nabla \times \mathbf{A}| = |\nabla A|$ in this geometry, we see that the nonlinearity of the problem is such that γ depends on $|\nabla A|$. It is convenient to consider γ to be a function of B^2, so that Eq. (29) written out in full becomes

$$(\gamma + 2\gamma' A_x^2)A_{xx} + 4\gamma' A_x A_y A_{xy} + (\gamma + 2\gamma' A_y^2)A_{yy} + 4\pi j = 0, \tag{30}$$

and (30) is elliptic if $\gamma + 2B^2\gamma' > 0$, or $d\mu/dB < \mu/B$, which is usually the case.

Equation (29) is equivalent to (1) with the current density playing the role of source term. Its finite difference approximation in a triangle mesh is therefore (16):

$$\sum_i w_i(A_i - A) + 4\pi I = 0, \tag{31}$$

where A_i, A now stand for the vector potential, and

$$I = \sum_{i=1}^{6} j_{i+1/2} a_{i+1/2} \tag{32}$$

is the total current through the secondary mesh dodecagon surrounding the vertex x,y at which A is defined.

The boundary conditions for the magnetic field require that at an interface the normal component of **B**, $\mathbf{B}_n$, and the tangential component of **H**, $\mathbf{H}_t$, be continuous. Because **A** has only a z-component, its gradient and curl are equal in magnitude and orthogonal to each other. Thus, expressed in terms of A,

$$\mathbf{H}_t = (\gamma \mathbf{B})_t = (\gamma \nabla \times \mathbf{A})_t = (\gamma \nabla A)_n$$

and

$$\mathbf{B}_n = (\nabla \times \mathbf{A})_n = (\nabla A)_t\,,$$

and we have already shown these to be continuous in our finite-difference approximation (Section III).

On external boundaries we assume a condition of no leakage of magnetic flux, so that $A = 0$. For symmetric magnets we calculate only one-half of the magnet and make the normal derivative of A equal to zero on the median plane by setting

all external coupling coefficients on the median plane equal to zero. Initial values of the vector potential are taken to be zero at all mesh points.

The method can be applied to any plane distribution of air, conductors, and

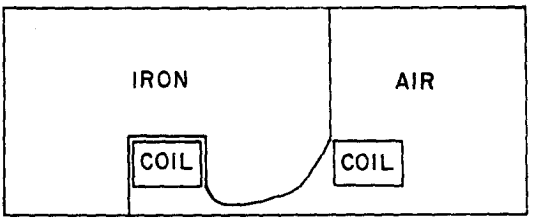

FIG. 3. *C*-Magnet showing material interfaces.

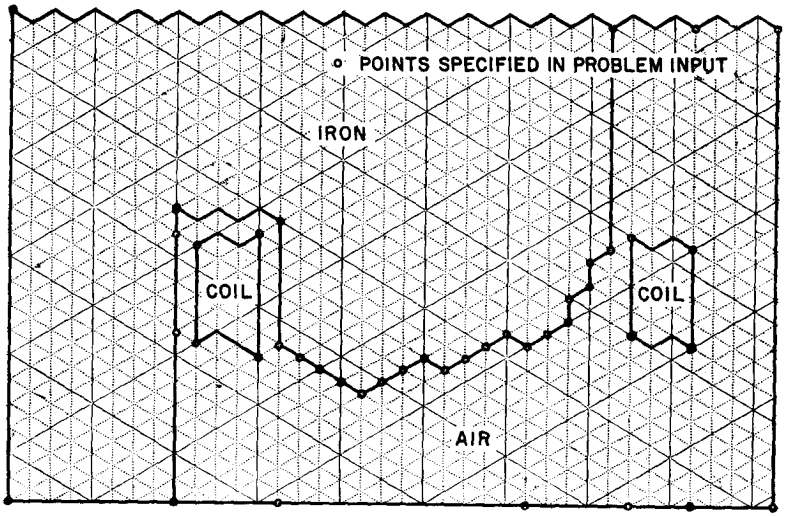

FIG. 4. Logical map of *C*-magnet mesh.

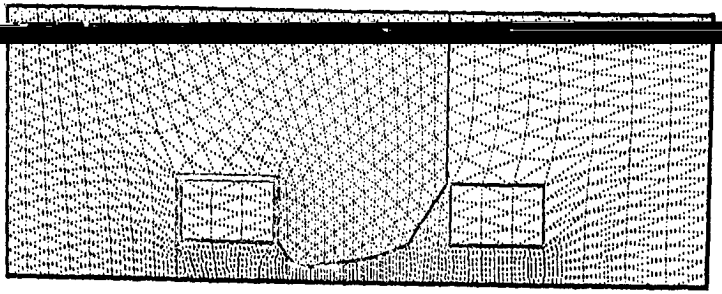

FIG. 5. *C*-Magnet showing triangle zones.

iron, and has been used to calculate the fields of various dipole, quadrupole, and sextupole magnets. Figures 3–11 show some results obtained for the CERN proton synchrotron *C*-magnet (open sector), a quadrupole, and a sextupole magnet. Equipotentials, which are also lines of force, have been drawn in by linear inter-

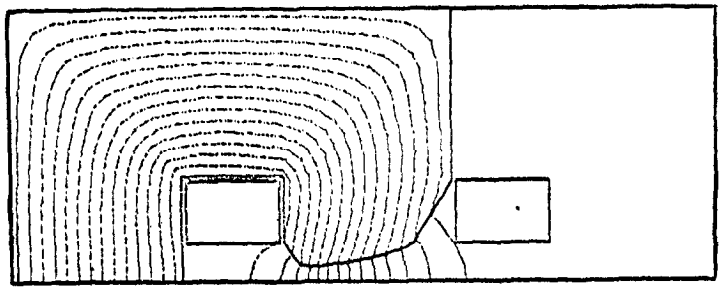

FIG. 6. *C*-Magnet showing equipotentials.

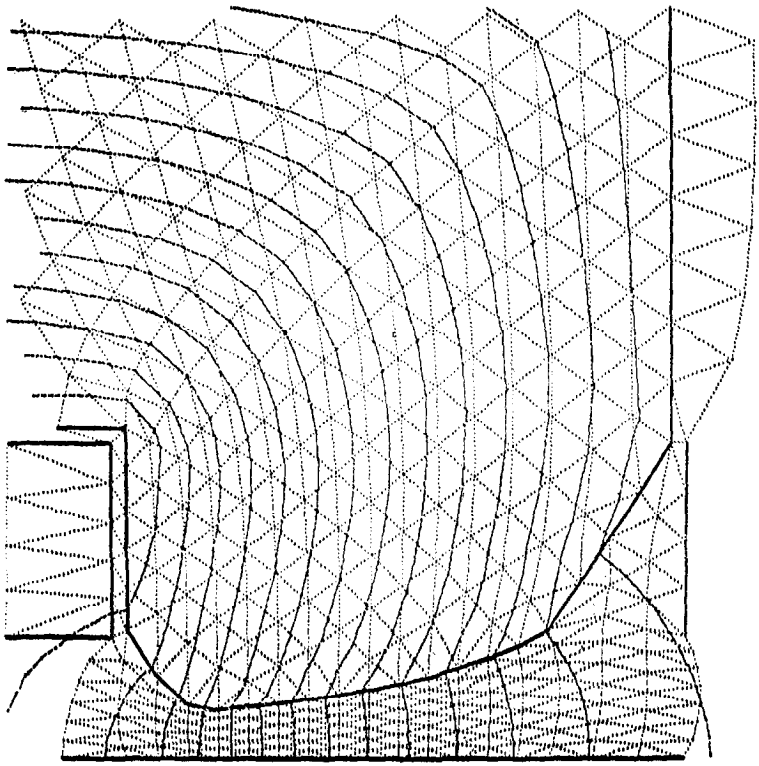

FIG. 7. Enlarged view of *C*-magnet.

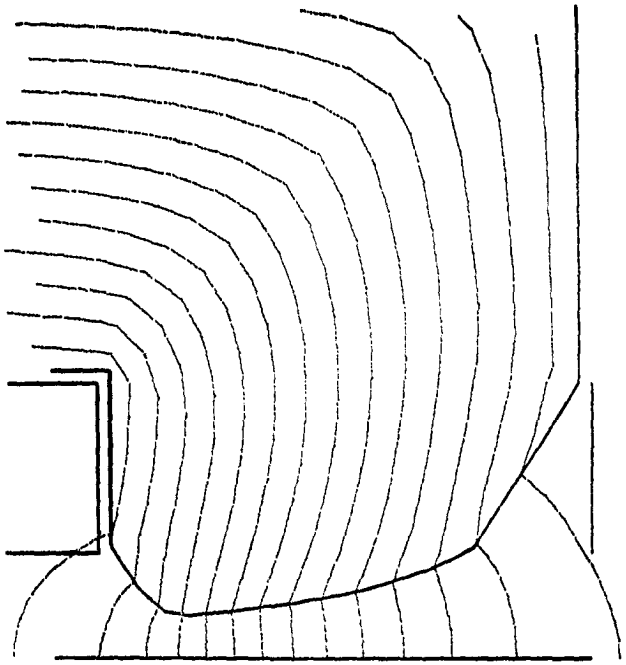

FIG. 8. Figure 7 without zone lines.

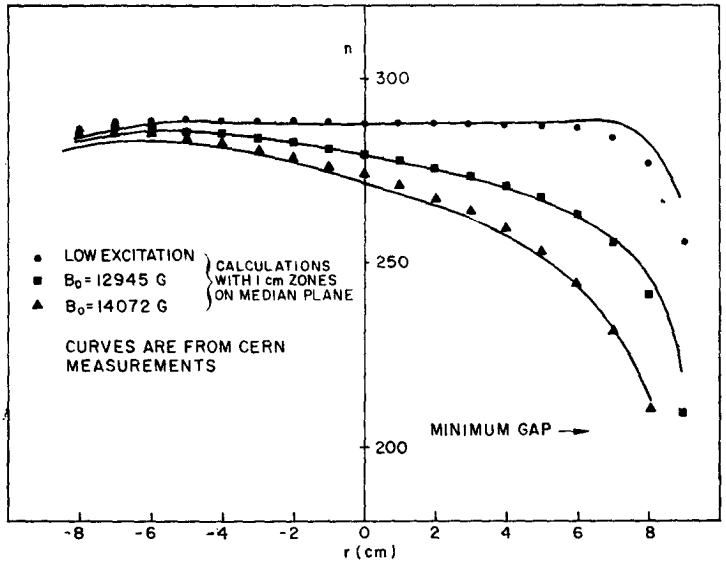

FIG. 9. n vs r for C-magnet ($n = |(R_0/B_0)\partial B/\partial r|$, $R_0 = 70.079$ m).

polation. The *C*-magnet results (which were obtained with a somewhat different mesh than that illustrated) agree with the experimental measurements of the field gradients to about 1% [16]. This accuracy is comparable with that obtained with other finite-difference calculations using rectangular meshes of about the same spacing [17]. (Theoretical studies of the discretization error of the solutions of (12) for linear problems may be found in [8] and [18]).

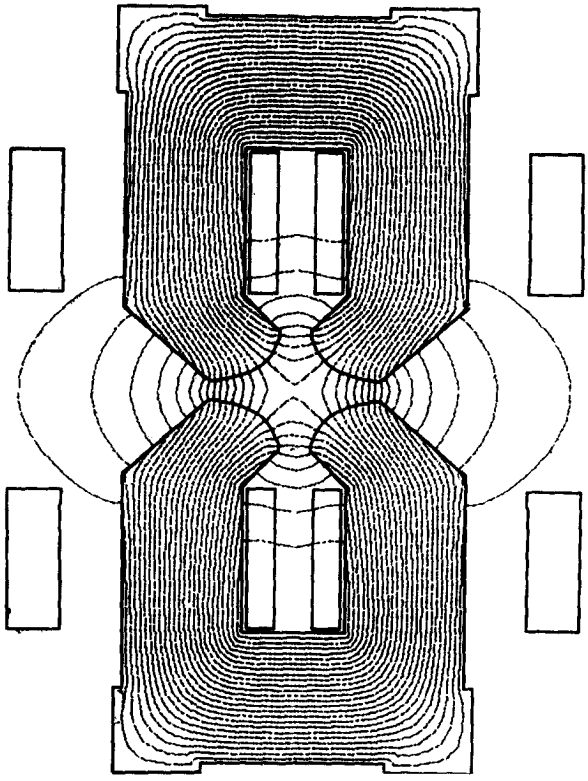

FIG. 10. A quadrupole magnet (from [16]).

Two methods can be used to obtain derivatives of the numerical solution: (a) right triangle zoning can be imposed in regions where the derivatives are desired, and derivatives can then be obtained by taking first and second differences parallel to the coordinate axes; (b) an interpolating polynomial can be fitted by least squares to each vertex and its neighbors, and then differentiated. The second method has the advantage of not requiring special zoning, and gives about the

same accuracy when employing harmonic polynomials as basis functions and solving by means of the generalized matrix inverse [19].

Using linearized overrelaxation, the calculating time with an IBM 7094 is 3 msec per mesh point per cycle for points in iron, and 0.6 msec for points not in iron. The optimized overrelaxation parameter usually lies between 1.90 and

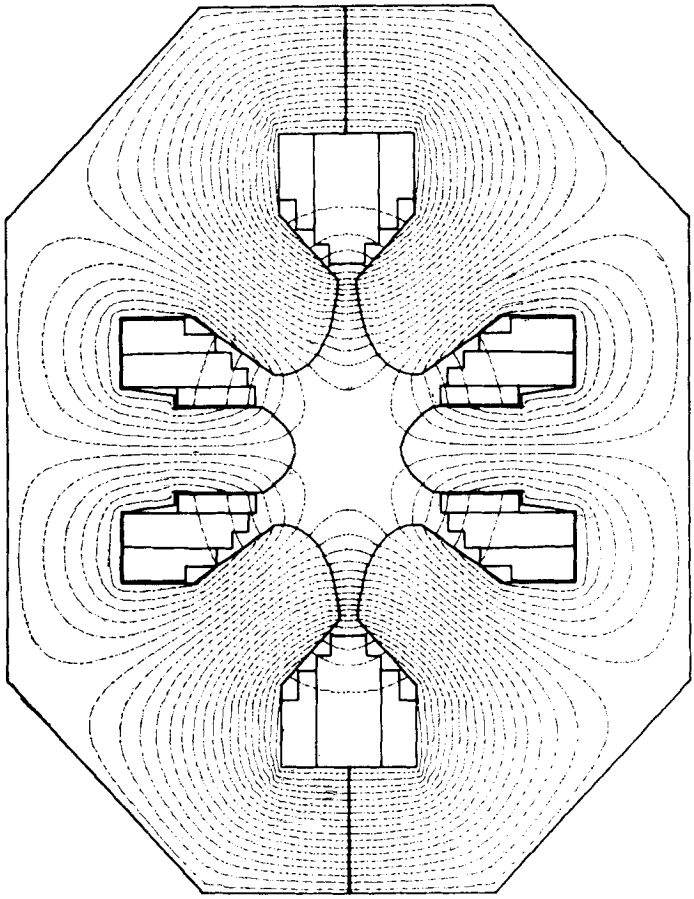

FIG. 11. A sextupole magnet (from [16]).

1.96, and from 200 to 800 cycles are usually required for convergence in a 40×40 mesh. Thus nonlinear problems with 1600 mesh points take 15–30 minutes to converge, while linear problems run about five times faster.

Nonlinear overrelaxation by Newton's method approximately doubles the

calculating time per iteration (in iron) and by Aitken's δ^2 method approximately triples it, but has been found by others [14] to reduce the number of iterations substantially in simple problems. Our experience thus far shows that, although Newton's method permits the optimum ω of (23) to be used both in air and iron, it requires about 50% more cycles to converge than the line-mixed method. With

6. Extension to Problems with Cylindrical Symmetry

The diffusion equation (2) and the magnetic field equation (29) with cylindrical symmetry can be treated in cylindrical coordinates r, z, θ by transforming to Cartesian coordinates.

Diffusion Equation

Let $\varphi = \varphi(r, z)$, independent of θ, and let ∇, ∇_c represent the del operator in Cartesian coordinates and cylindrical coordinates respectively. Then for any vector function $\mathbf{f}$ which is independent of θ we have

$$\nabla_c \cdot \mathbf{f} = \frac{1}{r} \nabla \cdot (r\mathbf{f}) .$$

Hence Eq. (2) becomes

$$\frac{1}{r} \nabla \cdot (r\lambda \nabla \varphi) = c \frac{\partial \varphi}{\partial t} .$$

We see that by replacing λ by $r\lambda$, and c by rc, we can treat the cylindrical coordinates z,r as if they were Cartesian coordinates x,y respectively.

In finite difference form we have in place of (6) and (8), respectively,

$$G = \sum_i c_{i+1/2} \bar{r}_{1+1/2} a_{i+1/2},$$

$$w_i = \tfrac{1}{2}(\lambda_{i+1/2} \bar{r}_{i+1/2} \cot\theta_{i+1/2} + \lambda_{i-1/2} \bar{r}_{i-1/2} \cot\theta_{i-1/2}),$$

where $\bar{r}_{i+1/2}$, the average radius of triangle $i + 1/2$, is given by

$$\bar{r}_{i+1/2} = \tfrac{1}{3}(r + r_i + r_{i+1})$$

and $\bar{\bar{r}}_{i+1/2}$ is the average radius of a quadrilateral at vertex r given by

$$\bar{\bar{r}}_{i+1/2} = \frac{7}{12}\bar{r}_{i+1/2} + \frac{5}{12}r.$$

Magnetic Field Equation

For a vector function $\mathbf{f}(r,z)$ which has only a θ-component we have

$$\nabla_c \times \mathbf{f} = \frac{1}{r}\nabla \times (r\mathbf{f}).$$

For a vector function $\mathbf{g}(r,z)$ which has only r- and z-components,

$$\nabla_c \times \mathbf{g} = \nabla \times \mathbf{g}.$$

Since $\mathbf{A}(r,z)$ and $\mathbf{j}(r,z)$ have only θ-components,

$$\mathbf{B} = \nabla_c \times \mathbf{A} = \frac{1}{r}\nabla \times (r\mathbf{A}).$$

Since $\mathbf{B}$ has only r- and z-components,

$$\nabla_c \times (\gamma\mathbf{B}) = \nabla \times (\gamma\mathbf{B}) = \nabla \times \left[\frac{\gamma}{r}\nabla \times (r\mathbf{A})\right] = 4\pi\mathbf{j}\,.$$

Thus (29) becomes

$$\nabla \cdot \left[\frac{\gamma}{r}\nabla(rA)\right] = -4\pi j\,.$$

We see that γ/r replaces γ, $r\mathbf{A}$ replaces $\mathbf{A}$, and $r\mathbf{B}$ replaces $\mathbf{B}$.

For a current loop, $A \sim r$ for small r, $A \sim 1/r^2$ for large r. Therefore the boundary conditions on rA are $rA \to 0$ as $r \to 0$ and $r \to \infty$.

7. Other Applications

The method presented here can be applied to elliptic equations which arise in other branches of physics. Some equations of this type can be regarded as special cases of the magnetostatic equation: for example, the restricted form of Plateau's minimal surface problem is equivalent to (1) with $\lambda = [1 + (\nabla\varphi)^2]^{-1/2}$ and $S = 0$. In others, such as the heat or diffusion equations, λ is a function of φ

rather than of $|\nabla\varphi|$, or is independent of φ. Applications have also been made to nuclear reactor problems [7] where S includes a term proportional to φ.

ACKNOWLEDGMENTS

The author wishes to thank C.F. Andrews for proposing application of this method to the magnetostatic problem and for helpful suggestions; R. Goldstein for developing the least squares program; and C.E. Leith for advice and encouragement.

APPENDIX. NUMERICAL CONSTRUCTION OF TOPOLOGICALLY REGULAR NONUNIFORM TRIANGLE MESHES

A nonuniform triangle mesh for an arbitrary polygonal boundary composed of arbitrarily shaped regions is most easily constructed by computer. In order to reflect the relative importance and the material properties of each region, the mesh for a given problem should also be composed of regions which can be zoned to different average mesh spacings, with the mesh spacing in each region varying smoothly. Linear interpolation can be used to distribute the mesh points along boundaries and interfaces, but this method is generally not useful for the interior points of regions of arbitrary shape.

A satisfactory method can be derived by formulating the zoning problem as a potential problem, with the mesh lines playing the role of equipotentials [20, 21]. The triangle mesh which we use can be mapped into a regular equilateral triangle array composed of three sets of straight lines intersecting each other at 60°, of which any two sets are sufficient to define the mesh. Let one of these two sets be associated with a function $\chi(x,y)$ and the other with a function $\psi(x,y)$ which satisfy the Laplace equations

$$\begin{aligned} \nabla^2\chi &= 0, \\ \nabla^2\psi &= 0 \end{aligned} \tag{33}$$

over each region with boundary conditions determined by the interface and boundary zoning. Solving (33), the intersecting "equipotentials" $\chi =$ constant and $\psi =$ constant, together with the third set drawn through the intersection points, form the desired triangle mesh. Because of the well-known averaging property of solutions to Laplace's equation, we might expect a mesh constructed in this way to be, in some sense, smooth.

Equations (33) can be solved numerically by inverting them and writing them in terms of $x(\chi, \psi)$ and $y(\chi,\psi)$. Using the relations

$$\chi_x = -\frac{1}{J} y_\psi \qquad \psi_x = \frac{1}{J} y_\chi$$

$$\chi_y = \frac{x_\psi}{J} \qquad \psi_y = -\frac{1}{J} x_\chi$$

where the Jacobian $J = x_\psi y_\chi - x_\chi y_\psi$, we find that (33) are transformed into the inverse Laplace equations

$$\begin{aligned} \alpha x_{\chi\chi} - 2\beta x_{\chi\psi} + \gamma x_{\psi\psi} &= 0, \\ \alpha y_{\chi\chi} - 2\beta y_{\chi\psi} + \gamma y_{\psi\psi} &= 0 \end{aligned} \tag{34}$$

wherever $J \neq 0$. Here α, β, γ are the quadratic functions

$$\begin{aligned} \alpha &= x_\psi^2 + y_\psi^2, \\ \beta &= x_\chi x_\psi + y_\chi y_\psi, \end{aligned} \tag{35}$$

and

$$\gamma = x_\chi^2 + y_\chi^2.$$

The solutions of the elliptic equations (34) give the coordinates of a given equipotential directly.

Finite-difference expressions for the derivatives occurring in (34) and (35) can be obtained by the line integral method using Gauss' theorem [22]. We use a path of integration around a given vertex which for the first derivatives passes through the six neighboring points and for the second derivatives follows the dodecagon in Fig. 1. Assigning values to χ and ψ which differ by unity on adjacent lines and vary linearly with position in χ,ψ space, we find

$$\begin{aligned} x_\chi &= \tfrac{1}{6}[(x_2 + 2x_1 + x_6) - (x_3 + 2x_4 + x_5)] \\ x_\psi &= \tfrac{1}{6}[(x_1 + 2x_6 + x_5) - (x_2 + 2x_3 + x_4)] \\ x_{\chi\chi} &= x_1 - 2x + x_4 \\ x_{\chi\psi} &= \tfrac{1}{2}[(x_1 + x_6 + x_3 + x_4) - (x_2 + x_5 + 2x)] \\ x_{\psi\psi} &= x_6 - 2x + x_3, \end{aligned} \tag{36}$$

and similarly for the derivatives of y, where x,y is the center point and we have identified χ with the lines 2–1, 3–6, 4–5, etc., and ψ with the lines 2–3, 1–4, 6–5, etc. (Fig. 12).

Substituting (36) into (34) and (35) we obtain for the finite-difference analogs of (34)

$$\sum_{i=1}^{6} c_i(x_i - x) = 0\,,$$
$$\sum_{i=1}^{6} c_i(y_i - y) = 0\,, \tag{37}$$

where $c_1 = c_4 = \alpha - \beta$, $c_2 = c_5 = \beta$, and $c_3 = c_6 = \gamma - \beta$.

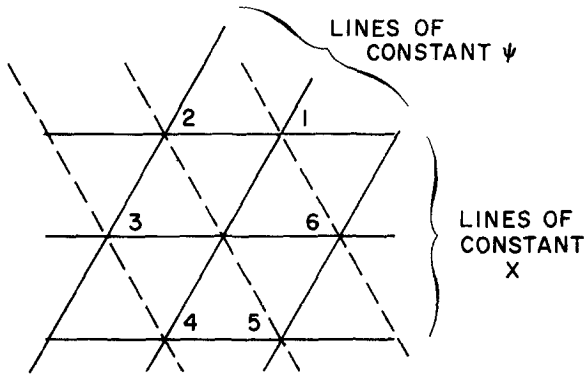

FIG. 12. A vertex and its six neighbors in χ, ψ space.

The nonlinear equations (37) can be solved by successive overrelaxation using automatic optimization as described in Section III with separate overrelaxation parameters for the x- and y-coordinates. The couplings c_i depend on the nearest-neighbor values x_i,y_i but not on x,y. Hence solving the equations

$$x = \frac{\sum_i c_i x_i}{\sum_i c_i}\,,$$
$$y = \frac{\sum_i c_i y_i}{\sum_i c_i} \tag{38}$$

in succession, recalculating the c_i at each mesh point, we have a sequence of linear problems which, in practice, converge rapidly, provided the initial approximation is satisfactory (see below). Figures 5 and 7 show a typical mesh obtained by this method. By the use of linear interpolation on boundaries and interfaces, only a relatively few points need be specified in the problem input (see Fig. 4).

The triangles produced in this way tend to be equilateral far away from boundaries; the c_i at each vertex become nearly equal and Eqs. (38) become

$$x = \tfrac{1}{6} \sum_i x_i ,$$
$$y = \tfrac{1}{6} \sum_i y_i . \tag{39}$$

At the same time $\alpha \approx \gamma$, $\beta \approx 0$, and (34) become

$$x_{\chi\chi} + x_{\psi\psi} \approx 0 ,$$
$$y_{\chi\chi} + y_{\psi\psi} \approx 0 \tag{40}$$

showing that x and y approximately satisfy Laplace's equation in χ,ψ space. Equations (39) were in fact the first to be used [5], and they produce a satisfactory mesh for convex regions, but near a concave boundary, the mesh lines tend to crowd together or even to fall outside the boundary. However, since Eqs. (39) are linear they can be used, starting for example with $x = y = 0$ at all interior mesh points, to provide an initial approximation for (37).

By redefining ψ to be a vertical zigzag line (for example 2, 3, 4 or 1,6, 5 in Fig. 12), a different set of weights c_i can be found which tend to produce right triangles [21]. Nonuniform quadrilateral meshes can also be constructed by this technique [20, 21].

References

1. R. Courant, *Bull. Am. Math. Soc.* **49**, 1 (1943).
2. L. Tasny-Tschiassny, *J. Appl. Phys.* **20**, 419 (1949).
3. R. H. MacNeal, *Quart. Appl. Math.* **11**, 295 (1953/54).
4. R. Grandey, Lawrence Radiation Laboratory, Livermore, California, 1957 (unpublished).
5. C. E. Leith, Lawrence Radiation Laboratory, Livermore, California, 1958 (unpublished).
6. A. M. Winslow, UCRL-7784, Lawrence Radiation Laboratory, Livermore, California (1964); and *Proceedings of the International Symposium on Magnet Technology* (H. Brechna and H. S. Gordon, eds.), p. 170. Stanford Linear Accelerator Center, Stanford, California, and Lawrence Radiation Laboratory, University of California, Berkeley, California (1965).
7. R. B. Kellog, Bettis Technical Review WAPD-BT-31, p. 51. Bettis Atomic Power Laboratory, Pittsburgh, Pennsylvania (1964).
8. K. O. Friedrichs, NYO-9760, Inst. for Math. and Sci., New York Univ., N.Y. (1962).
9. P. Rosen, *J. Appl. Phys.* **25**, 336 (1954); see also R. Courant and D. Hilbert, *Methods of Mathematical Physics*, Vol. II, p. 395. Wiley (Interscience), New York (1962).

10. J. L. SYNGE, *The Hypercircle in Mathematical Physics*, pp. 168–213. Cambridge Univ. Press, London (1957).

11. S. SCHECHTER, *Trans. Am. Math. Soc.* **104**, 179 (1962).

12. R. CHRISTIAN, private communication.

13. H. M. LIEBERSTEIN, MRC Tech. Summ. Report No. **80**, Math. Res. Center, U.S. Army

and *Proceedings of the International Symposium on Magnet Technology* (H. Brechna and H. S. Gordon eds.), p. 164. Stanford Linear Accelerator Center, Stanford, California, and Lawrence Radiation Laboratory, University of California, Berkeley, California (1965).

15. A. S. KRONROD, *Dokl. Akad. Nauk. SSR* **132**, 95 (1960).

16. J. S. COLONIAS and J. H. DORST, UCRL-16382, Lawrence Radiation Laboratory, Berkeley, California (1965).

17. J. H. DORST, UCRL-11798 and UCRL-16389, Lawrence Radiation Laboratory, Berkeley, California (1965).

18. R. B. KELLOGG, *Proceedings of the Conference on Computing Methods to Reactor Problems*, ANL–7050, p. 147, Argonne National Laboratory, Argonne, Illinois (1965).

19. T. N. E. GREVILLE, *J. Soc. Ind. Appl. Math.* **9**, 109 (1961).

20. W. P. CROWLEY, Memorandum, Lawrence Radiation Laboratory, Livermore, California (1962).

21. A. M. WINSLOW, UCRL-7312, Lawrence Radiation Laboratory, Livermore, California (1963).

22. W. F. NOH, in *Methods of Computational Physics* (B. J. Alder, S. Fernbach, and M. Rotenberg, eds.), Vol. III, p. 130. Academic Press, New York (1964).